Acta Metallomica – MEEMB, 2014, Tome XI, Nos. 2-4, 153-162

IS LYSINE 48 INVOLVED IN THE PROTONATION STEPS OF SUPEROXIDE REDUCTASE? A PRELIMINARY MOLECULAR DYNAMICS STUDY

Amr A.A. ATTIA*

Department of Chemistry, Faculty of Chemistry and Chemical Engineering, Babeş-Bolyai University, 11 Arany Janos, Cluj-Napoca, RO-400024, Romania

*E-mail: amrattia@chem.ubbcluj.ro

Preliminary classical molecular dynamics simulations were carried out to investigate the involvement of the proximal Lys residue (known in the literature as Lys_{48}) in the protonation steps of the ferric-(hydro)peroxo adduct of superoxide reductase. The results provided a general idea regarding the proximal Lys interaction with the active site and a possible role in the conformational changes to the adjacent residues towards the final one-electron reduction step in the catalytic cycle.

Key words: superoxide reductase, SOR, nonheme iron, molecular dynamics.

INTRODUCTION

Oxidative stress is among the most important phenomena in chemical biology. It is associated, in general, with an increased production of oxidizing species or a significant decrease in the cell's capability of antioxidant defenses. Such imbalance leads to a shift in the cell's redox state towards the oxidized state which could be destructive to living cells. The increased production of reactive oxygen species, including the one- and two-electron reductions of molecular oxygen, to superoxide and hydrogen peroxide respectively was found to contribute to DNA damage, lipid peroxidation, amino acids oxidation and can, in severe cases, provoke apoptosis. (Halliwell et al., 2007; Valentine et al., 1998; Brooker et al., 2011; Lennon et al., 1991).

As a defense mechanism against superoxide radicals, nearly all organisms living in the presence of oxygen contain isoforms of the superoxide scavenging enzyme superoxide dismutase (SOD), efficiently catalyzing the dismutation of superoxide to molecular oxygen and hydrogen peroxide which is further decomposed to water and molecular oxygen by the enzyme catalase (Mccord et al., 1996). Up until recently, the scavenging of superoxide, catalyzed by SODs, was considered the only biological mechanism for superoxide detoxification. However,

it has been discovered that some anaerobic bacteria and archaea, which might be accidentally exposed to molecular oxygen, protect themselves against harmful oxygen compounds through a different class of metalloenzymes, named superoxide reductases (SORs) (Jenney et al., 1999).

SOR is found to catalyze the reduction of superoxide to hydrogen peroxide at the diffusion level. The active site of SOR is comprised of a non-heme iron ion penta-coordinated to 4 equatorial histidines and an axial cysteine constituting the resting ferrous state. The resting ferric state on the other hand incorporates, in addition to the ferrous state structure, a carboxylate oxygen bound trans to the cysteine. (cf. Fig. 1). (Abreu et al., 2000; Jenney et al., 1999; Coulter et al., 2000; Lombard et al., 2000; Jovanovic et al., 2000; Rodrigues et al., 2007).

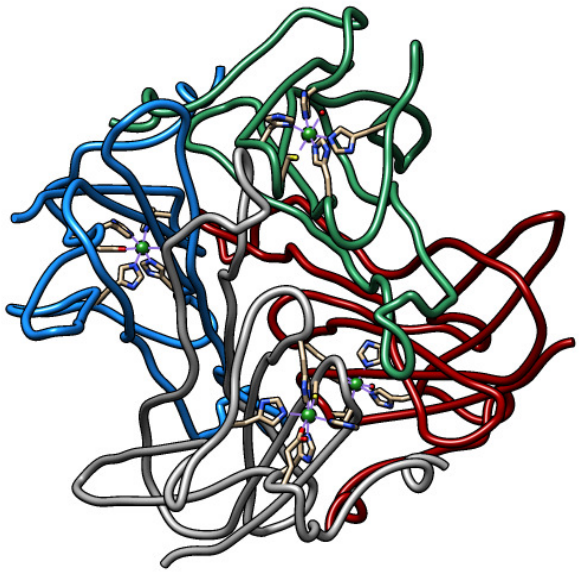

Fig. 1. The 1dqi pdb crystal structure of the tetrameric superoxide scavenging enzyme superoxide reduactase (SOR) from the anaerobic bacterium *Pyrococcus furiosus* (Yeh et al., 2000).

Fig. 2 illustrates the active site of SOR in the oxidized and reduced states highlighting the positions of the proximal Lys and Glu residues.

The generally accepted catalytic cycle of SOR is depicted in Fig. 3. Superoxide radical is proposed to bind to the active site forming a ferrous-superoxo/ferric-peroxo electromer followed by 2 subsequent protonation steps leading to ferric-hydroperoxo then ferric- hydrogen peroxide. The latter rapidly dissociates to yield the resting ferric state. The ferric state undergoes a one-electron reduction by the carboxylate terminal of the proximal Glu residue (Glu_{14} in Fig. 2) to regenerate the initial ferrous state (Kurtz Jr DM, 2004; Adams et al. 2002; Kurtz DM Jr, Coulter ED, 2002).

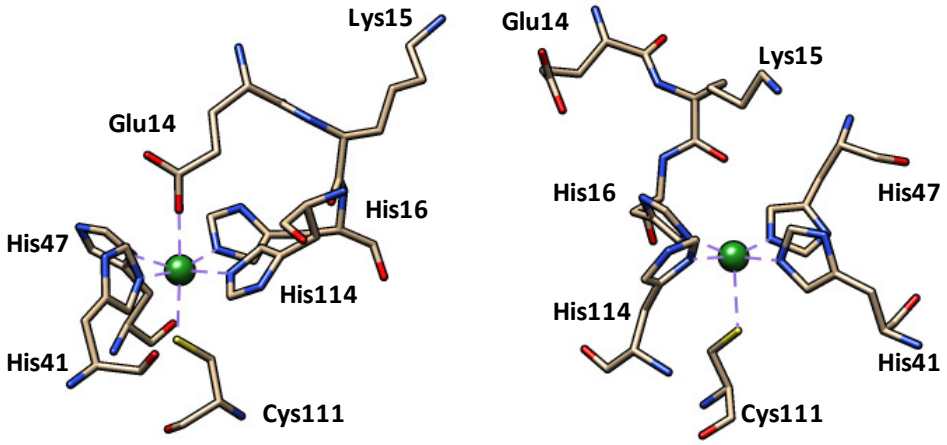

Fig. 2. Active site of SOR in the oxidized and reduced states shown on the right and the left respectively.

Though a considerable amount of studies have been reported on SORs, the identity of the reactive intermediate(s) in the catalytic cycle is still under debate (Lombard et al., 2001; Niviere et al., 2001). A pulse radiolysis study has previously established a reactive intermediate characterized by an absorption maximum at ~600 nm in the reaction of superoxide with ferrous SOR (Coulter et al., 2000; Emerson et al., 2002). This intermediate has been proposed by several reports as ferrous-superoxo, ferric-peroxo or ferric-hydroperoxo (Lombard et al., 2001; Niviere et al., 2001). The successful captivation of a ferric-(hydro)peroxo species in crystals of SOR was reported by Katona and co-workers in which the hydro(peroxo) moiety is bound in an end-on conformation (Katona et al., 2007).

Silaghi-Dumitrescu and co-workers have previously reported ZINDO/S-CI electronic absorption spectrum simulations and assigned the experimentally-observed 600-nm intermediate to a ferric-hydroperoxo species. The absorption maximum at 600 nm in such adduct was reported to arise from ligand to metal charge transfer – mainly thiolate to iron, with minor peroxide to iron contribution (Silaghi-Dumitrescu et al., 2003). More recently, the same group reported the first comparison of the energy profiles for Fe-O and O-O bond cleavage in ferric versus ferrous adducts of SOR with hydroperoxide and hydrogen peroxide. (Attia et al., 2013).

It has been generally suggested that two protonation steps are essential to convert superoxide to hydrogen peroxide in SORs. However, the source of the protons as well as the relation between the protonation and reduction steps are yet to be confirmed. The presence of the active site on the outer sphere of the enzyme would logically provide facile access to protons from water molecules thus shedding doubts on the involvement of Lys_{48} as a proton source. However, several

studies suggested that the proximal Lys_{48} residue plays a crucial role in the protonation steps of superoxide reduction in the catalytic cycle of SOR (Katona et al., 2007; Sit et al., 2010; Bonnot et al., 2012). In this study, preliminary classical molecular dynamics simulations provide a general interpretation of the degree of involvement of the proximal Lys residue in the protonation steps of SOR as well as the conformational changes of Lys alongside the adjacent Glu residue towards the final one-electron reduction step in the catalytic cycle.

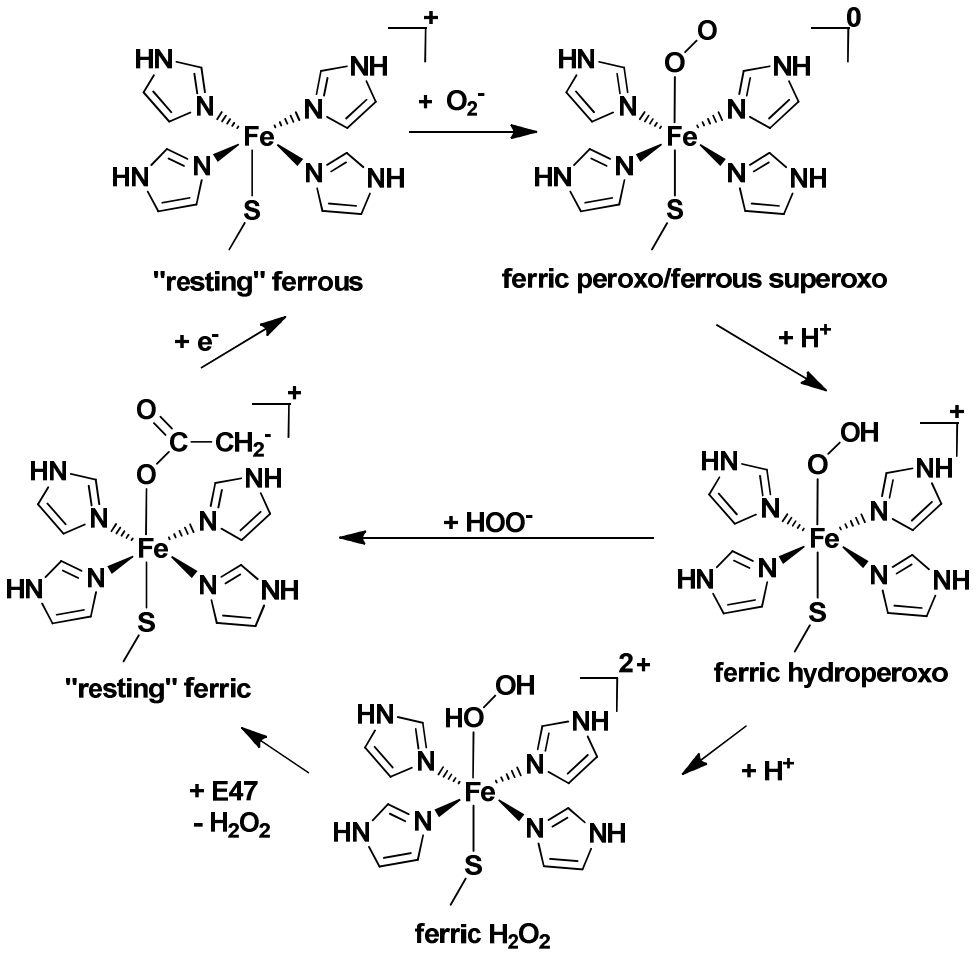

Fig. 3. Catalytic cycle proposed for superoxide reductases.

MATERIALS AND METHODS

Three chemical models were derived and constructed from the tetrameric SOR X-ray crystal structure of *Pyrococcus furiosus* (pdb id 1dqi). Models (**1**) and (**2**) are monomeric molecules each comprise a single SOR chain with the active site in the oxidized and reduced resting state respectively while model (**3**) is a dimer molecule serving as a combination of models (**1**) and (**2**), i.e. two adjacent SOR chains.

Molecular dynamics simulations (MD) were carried out using HyperChem 8 software package (Hypercube, 2011) employing the Amber99 force field (Wang A., 2000). The main scenarios investigated are those involving the proximal Lys residue or the proximal water molecules as sole proton sources, or a combination of both. Thus, all simulations were carried out both in vacuum and in water with no constraints (all atoms were allowed to move). For the simulations performed in water, a solvation box was constructed that constituted an estimated 3129 explicit water molecules for model (**1**), 3078 for model (**2**), and 5477 for the dimer model (**3**) with a minimum distance of 2.5 Å between the water molecules and the enzyme in each case. Minimization calculations were performed on all structures prior to the MD runs. The distance trajectories between the ferric center and both the side chain terminal of the proximal Lys (denoted as NLys) and the carboxylate terminal of the proximal Glutamate (denoted as OGlu) are recorded and discussed. The simulations were carried out over the course of 22 ps with a step size of 1 fs. The simulation temperature was set to 370 K as the present crystal structure is derived from a thermophile organism; it should be noted however that SOR is found to be active at much lower temperatures as well (Katona et al., 2007; Sit et al., 2010; Bonnot et al., 2012). In the X-ray crystal structure employed in this study, the proximal Lys residue referred to in the literature as Lys_{48} is denoted Lys_{15} according to the ordering of the residues.

RESULTS AND DISCUSSION

Fig. 4 illustrates the results obtained from MD simulations performed on Model (**1**). After a simulation time of 22 ps, the distance between Fe and N_{Lys15} decreased from an initial 5.7 to 2.9 Å in case of the solvated simulation whereas it increased to approximately 10.5 Å in vacuum. On the other hand, as shown in Fig. 5, the distance between Fe and O_{Glu14} decreased from an initial 11.5 Å to 10.3 Å in vacuum and further to 6.3 Å in the event of the simulation carried out in water.

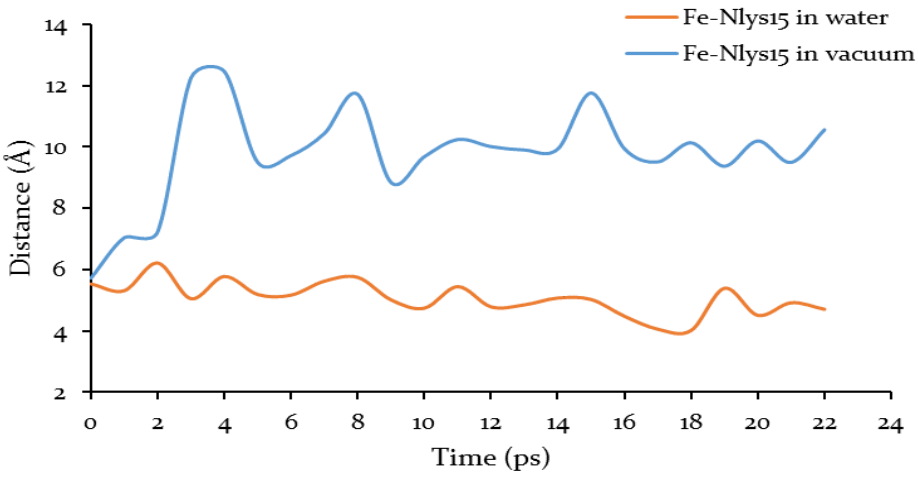

Fig. 4. The evolution of the distance between Fe and N of Lys_{15} in model (**1**) of 1dqi SOR as obtained from MD simulations in vacuum and in water.

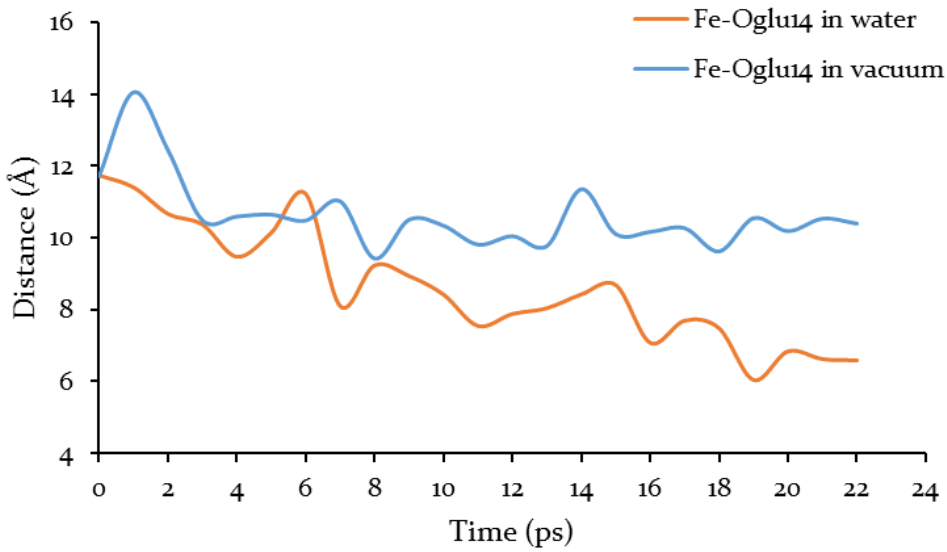

Fig. 5. The evolution of the distance between Fe and O_{Glu14} in model (**1**) of 1dqi SOR as obtained from MD simulations in vacuum and in water.

Fig. 6 depicts the distance between Fe and N_{Lys15} in model (**2**) (where Glu_{14} is bound to the active site and Fe is in the resting ferric state). No major changes in distances were observed at the end of the simulations, being only in the range of 1 Å in both vacuum and water cases.

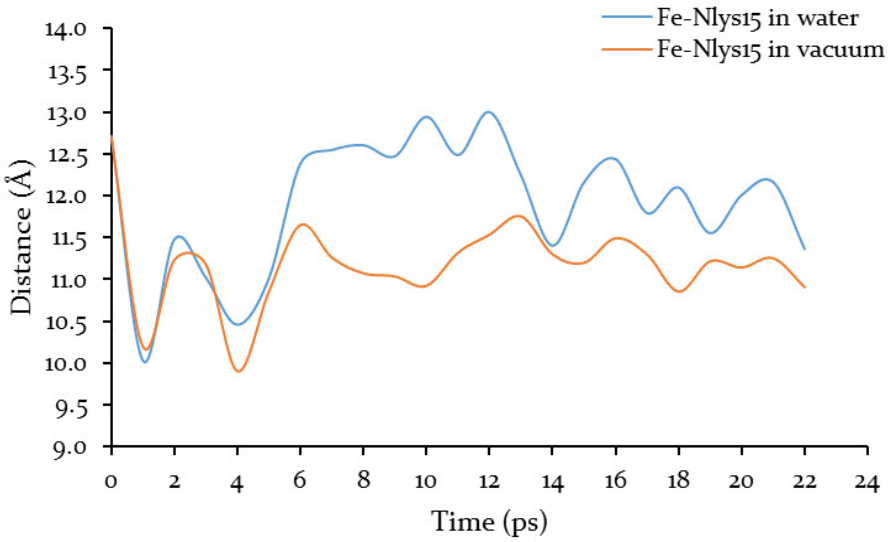

Fig. 6. The evolution of the distance between Fe and N_{Lys15} in model (**2**) of 1dqi SOR as obtained from MD simulations in vacuum and in water.

The Fe-N_{Lys} and Fe-O_{Glu} trajectories examined so far were obtained from simulations on monomer chains (models **1** and **2**) however, since SOR is in fact a tetramer enzyme the influence of the neighboring chains on such trajectories should not be overlooked. Figs 7 and 8 show a comparison between the Fe-Nlys and Fe-Oglu trajectories resulted from monomer simulations (model **1**) versus the same trajectories obtained from simulations performed on a dimer system (model **3**). As seen in Fig. 7, both Fe-N_{lys15} trajectories were found within 1 Å at the end of the simulation. Conversely, the evolution of the Fe-O_{glu14} distances was dissimilar, it can be observed in Fig. 8 that a difference of almost 4 Å between both cases is visible. Similar trends were obtained in the solvated simulations (results not shown).

The results represented above suggest the involvement of Lys in the protonation steps of SOR either through the direct interaction with the (hydro)peroxo ligand or indirectly through hydrogen bonding network with the water molecules at the vicinity of the active site. Indeed the solvent exposed active site, with an abundance of protons, would shed some doubts on such involvement. Conversely, a recent study has shown that the mutation of Lysine48 to the hydrophobic amino acid Isoleucine was found to give rise to O-O bond cleavage and formation of a high-valent iron adduct compared to the wild type. Though such study was performed on the ferrous-hydroperoxo SOR species rather than the ferric form, the role of Lys_{48} in stabilizing the hydroperoxo adduct and thus preventing O-O bond cleavage was greatly stressed. (Bonnot et al., 2012).

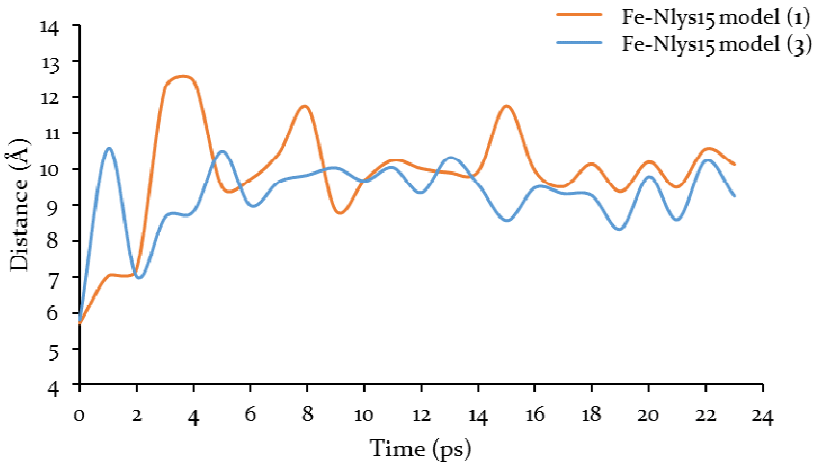

Fig. 7. The evolution of the distance between Fe and N_{Lys15} in model (**1**) versus that in model (**3**) as obtained from MD simulations in vacuum.

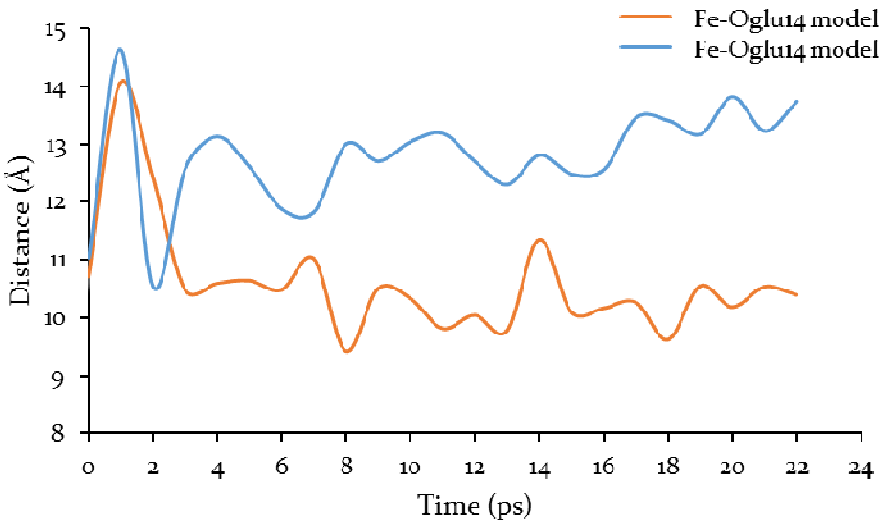

Fig. 8. The evolution of the distance between Fe and O_{Glu14} in model (**1**) versus that in model (**3**) as obtained from MD simulations in vacuum.

Additionally, The Fe-Lys and the Fe-Glu distances obtained from the MD simulations can be interpreted as an interesting case of position alternations between Lys and Glu. This would suggest a possible role of Lys, beyond that of a proton donor, in providing the necessary conformational changes to the proximal peptide chain to allow the interaction between Glu and the ferric active site for the

final reduction step to take place. This latter suggestion can be verified by additional computations on versions of the enzyme where Lys and/or Glu are replaced by other residues. These computations are currently in the works.

Acknowledgements: Funding from the Romanian Ministry of Education and Research (Grant PN-II-ID-PCE-2012-4-0488) is gratefully acknowledged. Dr. R. Silaghi-Dumitrescu (UBB) is thanked for helpful discussions.

REFERENCES

1. Abreu I.A., Saraiva L.M,. Carita J., Huber H, Stetter K.O., Cabelli D.E., Teixeira M. – Oxygen detoxification in the strict anaerobic archaeon Archaeoglobus fulgidus: superoxide scavenging by neelaredoxin, Mol. Microb., 2000, 38, 322-334.
2. Adams M.W., Jenney F.E. Jr., Clay M.D., Johnson M.K. – Superoxide reductase: fact or fiction?, J. Biol. Inorg. Chem., 2002, 7, 647-652.
3. Attia A.A., Cioloboc D., Lupan A., Silaghi-Dumitrescu R. – Fe-O versus O-O in reactive iron peroxide intermediates of superoxide reductase, J. Biol. Inorg. Chem., 2013, 18, 95-101.
4. Bonnot F., Molle T., Menage S., Moreau Y., Duval S., Houee-Levin C., Niviere V. – Control of the evolution of iron peroxide intermediate in superoxide reductase from *Desulfoarculus baarsii*. Involvement of lysine 48 in protonation, J. Am. Chem. Soc., 2012, 134, 5120-5130.
5. Brooker R.J. – *Genetics: analysis and principles* 4th ed., 2011, McGraw-Hill Science. ISBN 978-0073525280.
6. Coulter E.D., Emerson J.P., Kurtz Jr. D.M., Cabelli D.E. – Superoxide Reactivity of Rubredoxin Oxidoreductase (Desulfoferrodoxin) from *Desulfovibrio vulgaris*: A Pulse Radiolysis Study, J. Am. Chem. Soc., 2000, 122, 11555-11556.
7. Emerson J.P., Coulter E.D., Cabelli D.E., Phillips R., Kurtz D.M. Jr. – Kinetics and mechanism of superoxide reduction by two-iron superoxide reductase from *Desulfovibrio vulgaris*, Biochemistry, 2002, 41, 4348-4357.
8. Halliwell B. – Biochemistry of oxidative stress, Biochemical Society Transactions, 2007, 35,1147-1150.
9. Hyperchem. HyperChem(TM) Molecular Modelling System, Release 8.0 for Windows, Hypercube, Inc. 2011.
10. Jenney F.E., Verhagen M.F., Cui X.Y., Adams W.W. – Anaerobic microbes: oxygen detoxification without superoxide dismutase, Science, 1999, 286, 306-309.
11. Jovanovic T., Ascenso C., Hazlett R. O., Sikkink R., Krebs C., Litwiller R., Benson L.M., Moura I., Moura J.G., Radolf J.D., Huynh B., Naylor S., Rusnak F. – Neelaredoxin, an iron-binding protein from the syphilis spirochete, Treponema pallidum, is a superoxide reductase, J. Biol. Chem., 2000, 275, 28439-28448.
12. Katona G., Carpentier P., Niviere V., Amara P., Adam V., Ohana J., Tsanov N., Bourgeois D. – Raman-assisted crystallography reveals end-on peroxide intermediates in a nonheme iron enzyme, Science, 2007, 316, 449-453.
13. Kurtz Jr. D.M. – Microbial detoxification of superoxide: the non-heme iron reductive paradigm for combating oxidative stress, Acc. Chem. Res., 2004, 37, 902-908.
14. Kurtz D.M. Jr, Coulter E.D. – The mechanism(s) of superoxide reduction by superoxide reductases in vitro and in vivo, J. Biol. Inorg. Chem., 2002, 7, 653-658.
15. Lennon S.V., Martin S.J., Cotter T.G. – Dose-dependent induction of apoptosis in human tumour cell lines by widely diverging stimuli, Cell Prolif., 1991, 24:203-14.

16. Lombard M., Houee-Levin C., Touati D., Fontecave M., Niviere V. – Superoxide reductase from Desulfoarculus baarsii: reaction mechanism and role of glutamate 47 and lysine 48 in catalysis, Biochemistry, 2001, 40, 5032-5050.
17. Lombard M., Fontecave M., Touati D., Nivière V. – Reaction of the desulfoferrodoxin from Desulfoarculus baarsii with superoxide anion. Evidence for a superoxide reductase activity, J. Biol. Chem., 2000, 275, 115-121.
18. Mccord J.M., Fridovich I. – Superoxide dismutase. An enzymic function for erythrocuprein (hemocuprein), J. Biol. Chem. 1996, 22, 6049-6051.
19. Nivière V., Lombard M., Fontecave M., Houee-Levin C. – Pulse radiolysis studies on superoxide reductase from Treponema pallidum, FEBS Lett., 2001, 497, 171-173.
20. Rodrigues J.V., Saraiva L.M., Abreu I.A., Teixeira M., Cabelli D.E. – Superoxide reduction by Archaeoglobus fulgidus desulfoferrodoxin: comparison with neelaredoxin, J. Biol. Inorg. Chem., 2007 12:248-256.
21. Silaghi-Dumitrescu R., Silaghi-Dumitrescu I., Coulter E.D., Kurtz D.M. – Computational study of the non-heme iron active site in superoxide reductase and its reaction with superoxide, J. Inorg. Chem., 2003, 42, 446-456.
22. Sit P.H., Migliore A., Ho M.H., Klein M.L. – Quantum Mechanical and Quantum Mechanical/Molecular Mechanical Studies of the Iron−Dioxygen Intermediates and Proton Transfer in Superoxide Reductase, J. Chem. Theory. Comput., 2010, 6, 2896-2909.
23. Valentine J.S., Wertz D.L., Lyons T.J., Liou L.L., Goto J.J., Gralla E.B. – The dark side of dioxygen biology, Curr. Opin. Chem. Biol., 1998, 2:253-262.
24. Wang A. – How well does a restrained electrostatic potential (RESP) model perform in calculating conformational energies of organic and biological molecules?, J. Comp. Chem., 2000, 21, 1049-1074.
25. Yeh A.P., Hu Y., Jenney F.E., Adams M.W., Rees D.C. – Structures of the superoxide reductase from Pyrococcus furiosus in the oxidized and reduced states, Biochemistry 2000, 39, 2499-2508.